





Article

Pea and Soy Protein Stabilized Emulsions: Formulation, Structure, and Stability Studies

Eleni Galani ^{1,2}, Isabelle Ly ³, Eric Laurichesse ³, Veronique Schmitt ³, Aristotelis Xenakis ¹
and Maria D. Chatzidaki ^{1,*}

¹ Institute of Chemical Biology, National Hellenic Research Foundation, 11635 Athens, Greece

² Food Chemistry & Human Nutrition, School of Food, Biotechnology and Development, Agricultural University of Athens, 11855 Athens, Greece

³ CNRS Centre de Recherche Paul Pascal, University of Bordeaux, 33600 Bordeaux, France

* Correspondence: mhatzidaki@eie.gr

Abstract: During the last decades, there has been a huge consumer concern about animal proteins that has led to their replacement with plant proteins. Most of those proteins exhibit emulsifying properties; thus, the food industry begins their extensive use in various food matrices. In the present study, pea and soy protein isolates (PPI and SPI) were tested as potential candidates for stabilizing food emulsions to encapsulate α -tocopherol and squalene. More specifically, PPI and SPI particles were formulated using the pH modification method. Following, emulsions were prepared using high-shear homogenization and were observed at both a microscopic and macroscopic level. Furthermore, the adsorption of the proteins was measured using the bicinchoninic acid protein assay. The emulsions' droplet size as well as their antioxidant capacity were also evaluated. It was found that the droplet diameter of the SPI-based emulsions was 60.0 μm , while the PPI ones had a relatively smaller diameter of approximately 57.9 μm . In the presence of the bioactives, both emulsions showed scavenging activity of the 2,20-Azinobis-(3-ethylbenzothiazoline-6-sulphonate) radical cation (ABTS^{•+}) and 2,2-diphenyl-1-picrylhydrazyl (DPPH) radicals, with the ones loaded with α -tocopherol having the greatest antioxidant capacity. Overall, the proposed systems are very good candidates in different food matrices, with applications ranging from vegan milks and soups to meat alternative products.

Keywords: pea protein isolate; soy protein isolate; food emulsions; particle-stabilized emulsions



Citation: Galani, E.; Ly, I.; Laurichesse, E.; Schmitt, V.; Xenakis, A.; Chatzidaki, M.D. Pea and Soy Protein Stabilized Emulsions: Formulation, Structure, and Stability Studies. *Colloids Interfaces* **2023**, *7*, 30. <https://doi.org/10.3390/colloids7020030>

Academic Editors: Eleni P. Kalogianni, Julia Maldonado-Valderrama and Reinhard Miller

Received: 26 January 2023

Revised: 17 March 2023

Accepted: 31 March 2023

Published: 6 April 2023



Copyright: © 2023 by the authors. Licensee MDPI, Basel, Switzerland. This article is an open access article distributed under the terms and conditions of the Creative Commons Attribution (CC BY) license (<https://creativecommons.org/licenses/by/4.0/>).

1. Introduction

The modern food industry is facing an increasing demand for healthier and more sustainable food options. As the human population grows, the production of processed foods from animal sources is increasing. Unfortunately, this type of diet often contains saturated fats and results in diet-related diseases, such as obesity and diabetes [1,2], or has led to the outbreak of infectious diseases and antibiotic resistance [3]. Moreover, the increased demand for animal products, such as milk, eggs, and meat, has a huge effect on the environment and raises many ethical issues concerning animal welfare [4]. According to the suggestions of the EAT-Lancet commission, there should be a significant decrease on the consumption of animal-derived products by 2030 [5]. For the specific case of dairy products, allergies as well as lactose intolerance have led consumers to search for healthier alternatives. The commercial milk-alternative products based on coconut, soy, almond, and other sources are poorly accepted by the consumers due to the differences in quality, organoleptic characteristics, and functional attributes, such as stability, creaming, undercooking, etc. [6]. Most of the plant proteins currently used in the food industry are derived from wheat or soybeans. Nevertheless, due to the allergenicity of both ingredients and consumer demand for alternative options, there is an increasing interest in the use of proteins from peas, faba beans, rice, and other plants. Even though soybean may face some

challenges since it is listed as a food allergen [7], it remains one of the most promising plant proteins in terms of stability and functionality. More specifically, soybean proteins have shown important functional properties such as emulsifying, wetting, and/or gelling [8]. Pea protein has also been found to show important properties when used in food matrices [9]. These important properties have made soybean and pea proteins acceptable as alternatives to animal proteins in the food industry, especially in products such as plant-based milks or even meat-analog products [10,11].

Among the technological strategies used to design and develop these novel products are those based on structural modifications of food systems. This could be accomplished by changes in the pH, temperature, solubility, and other parameters to improve the texture and mouthfeel of the end product. Emulsions are systems widely used for the development of food products. However, in the past decades, one specific type of emulsion has received increasing interest, namely particle-stabilized emulsions. Ramsden and Pickering were the first to study the interfacial phenomena taking place in these emulsions, and independently observed that solid particles were able to stabilize the interface between two immiscible liquids [12,13]. Particle stabilized emulsions have the great benefit of being surfactant-free, and functional particles with high nutritional value, such as proteins, lipids, polysaccharides, etc., can be used as stabilizers [14]. The peculiarity of these types of emulsions is that the particles used are partially wettable, both by the water and the oil phases, and they are adsorbed at the oil-water interphase, forming a steric barrier, that prevents oil and water from coming into contact, thus stabilizing the emulsion droplets [15,16]. In this respect, protein-based emulsions have been proposed as versatile systems with tunable characteristics [17,18] that could act as good candidates for food applications.

These systems also have the ability to entrap bioactives with different solubilities, giving the final product health benefits. Such valuable bioactive compounds are α -tocopherol, widely known as vitamin E, and squalene. α -tocopherol is a plant-derived, lipid-soluble essential micronutrient and has been used in various fields, including pharmaceuticals, cosmetics, and foods [19–22]. α -tocopherol has been found to play an important role in the maintenance of good health as well as the prevention and/or treatment of some diseases and disorders. The recommended daily intake is 15 mg (22.4 IU, International Unit) for adults [23]. Multiple functions of α -tocopherol have been reported, including antioxidant activity by scavenging free radicals, membrane stabilization by forming complexes with destabilizing molecules, regulation of enzyme activity, and prevention of diseases, including neurological disorders, cardiovascular diseases, and age-related skin damage [24–26]. Among these functions, the role of α -tocopherol as an antioxidant against free radicals has been unequivocally demonstrated and it appears that this is the most important function of α -tocopherol. α -tocopherol also inhibits air oxidation of foods and oils, expanding their shelf-life [27,28]. Squalene is a natural triterpene, and a lipid that acts as a precursor to the biosynthesis of sterols, including cholesterol. It is widely found in nature, and especially in vegetable oils, such as olive oil. Squalene has several beneficial properties. It is a natural antioxidant, serves in skin hydration, and has been used as an emollient in vaccines [29–31]. As a compound of olive oil, it has also been studied for anticancer and cardio-protective properties, while it decreases the cholesterol level [32–34]. In countries around the Mediterranean Sea, a high squalene consumption was observed (200–400 mg per day) through the intensive use of olive oil. Since squalene is not approved by the FDA for treating any conditions, there is no official dose. Users and supplement manufacturers have established unofficial doses based on trial and error. The average intake of squalene is estimated to be around 30 mg per day [35]. However, when olive oil plays a more prominent role in the diet, such as the Mediterranean diet, levels of squalene can reach anywhere from 200 to 400 mg per day. Shark liver oil supplements commonly contain between 120 to 500 mg of squalene per dose. Studies have indicated that squalene supplements are tolerable up to 27 g with mild side effects [36].

The aim of the present study is to examine the formation of particles from pea or soy protein isolates that would stabilize oil-in-water emulsions for food applications. In these

emulsions, α -tocopherol or squalene were encapsulated to enhance the system's antioxidant capacity while increasing the health benefits of the system. Overall, the proposed systems could be good candidates for novel food applications.

2. Materials and Methods

2.1. Materials

Pea protein isolate (NUTRALYS® F85F) ($\geq 83\%$ protein content) was purchased from Roquette, France. Soy protein isolate ($\geq 90\%$ protein content) was purchased from Ingretia Global Trading LLC (Miami, FL, USA). Acetic acid, sodium hydroxide, 2,2-diphenyl-1-picrylhydrazyl (DPPH), 2,20-Azinobis-(3-ethylbenzothiazoline-6-sulphonate) (ABTS), α -tocopherol and potassium persulfate were purchased from Sigma-Aldrich (Chemie GmbH Munich, Germany). The bicinchoninic acid assay kit (BCA) and Squalene (98%) were purchased from Thermo Fisher Scientific, (Waltham, MA, USA). Mygliol 812N (MCT) was purchased from IOI Oleochemical (Penang, Malaysia). Extra virgin olive oil (EVOO) and sunflower oil (SFO) were purchased from a local supermarket.

2.2. Experimental Design

2.2.1. Preparation of Particles

Both kinds of particles were prepared at four different concentrations, namely 0.1, 0.2, 0.3, and 0.5% *w/v*. This was in order to evaluate the ability of the particles to formulate emulsions and choose the most suitable to proceed with the rest of the experiments.

Pea Protein Isolate (PPI) Particles

The preparation of PPI particles was based on the previous study by Liang et al., (2014) [37], with some modifications. More specifically, native PPI was measured in glass vials in proper quantities to achieve the concentrations previously mentioned. Afterwards, the required volume of deionized water was added and then the dispersions were stirred for 30 min using a magnetic stirrer. Subsequently, as recommended by Liang et al., the pH was adjusted to 3.0, using HCl 1 M. The dispersions remained under magnetic stirring for 2 h and were finally stored overnight at 4 °C to allow the complete hydration of the proteins [37].

Soy Protein Isolate (SPI) Particles

Particles were prepared from native SPI using a variation of the method used by Jiang et al., (2009) [38]. In this method, proper quantities of SPI were dispersed in the required volume of deionized water, and the dispersions were placed under magnetic stirring for 30 min. Afterwards, the dispersions' pH was shifted to 3.0 with HCl 1 M, and the dispersions remained under magnetic stirring for 2 h. Following that, pH was adjusted to 7.0 to induce the refolding of the proteins, and the magnetic stirring was carried on for one more hour [38].

Both the PPI and SPI particles were stored in the fridge to avoid microbiological growth.

2.2.2. Determination of Particles' Dimensions and ζ -Potential by Dynamic Light Scattering (DLS)

A Zetasizer Nano ZS (ZEN3600) analyzer (Malvern Instruments Ltd., Malvern, UK) equipped with a He-Ne laser (633 nm) and non-invasive backscatter (NIBS) optics was used for initial particle size measurements of the SPI and PPI dispersions. The polydispersity index (PDI) of the particles was also determined. All samples were diluted to 0.01 mg/L, and the pH was readjusted, if necessary, because dilution with distilled water can affect the pH. For the ζ -potential measurements, no dilution was needed. For comparative purposes, the size of soluble proteins of PPI and dispersions prior to pH modification. For this, PPI and SPI were dispersed in water for 30 min. The dispersions were centrifuged to remove any insoluble parts ($8000 \times g$, 15 min), and the supernatant was diluted 500 times. Results were processed with the Malvern Zetasizer Nano software, version 6.32 (Malvern

Instruments Ltd., Malvern, UK), which fits a spherical model of diffusing particles with low polydispersity. Measurements were carried out in triplicate at 25 °C [39].

2.2.3. Morphology Observation of Particles by Freeze-Fracture Transmission Electron Microscopy (FFTEM)

Freeze-fracture (FF) replica preparation was performed by putting a drop of the sample onto a gold planchette, then freezing the sample by quickly plunging the holder into liquid propane that was held at the temperature of liquid nitrogen. The freezing step must be fast in order to vitrify the sample and avoid structure disruption due to crystallization. Frozen samples were then introduced in the freeze-fracture enclosure of a BAF 060 Leica Microsystems apparatus held at a temperature of -50 °C and a pressure of 10^{-8} mBar. The samples were fractured using a metal knife held at a temperature of -200 °C. The fractured surface was immediately shadowed by the successive deposition of platinum at an angle of 45° and carbon at an angle of 90° . Outside the BAF060, the gold planchettes were immersed in the sample solution to detach the replicas from the samples. These replicas were then immersed in several consecutive baths of ethanol and NaOH (1M) in order to destroy the left sample, and finally in pure water for a few more hours. The replicas were finally collected on 400 mesh copper grids and dried before transmission electron microscopy (TEM) imaging. TEM was performed with a HITACHI H 600 microscope operating at 75 kV [40].

2.3. Analytical Measurements

For the present work, two O/W emulsions were prepared and stabilized by SPI or PPI particles. For the preparation, the particles' dispersions (0.1, 0.2, 0.3, and 0.5% *w/v*), deionized water, acted as the aqueous phase, and EVOO as the oil phase. Both empty and loaded emulsions were prepared, with the loaded ones containing α -tocopherol or squalene as the encapsulated substance (1% *w/w*). α -tocopherol and squalene were dissolved in EVOO by magnetic stirring. To ensure the best dispersion in EVOO, the mixture was kept under stirring at 800 rpm for 20 min. EVOO containing the bioactives was then incorporated in the systems in the way presented below in Section 2.3.1. Furthermore, different water:oil ratios were examined, namely 80:20, 70:30, and 60:40 *w/v*, to assess the highest quantity of oil that can be encapsulated by each emulsion.

2.3.1. Preparation of Emulsions

The preparation method was based on the previously published work by Mwangi et. al., (2016) [41]. More specifically, the aqueous phase was measured in a glass vial followed by the stepwise addition of the oil, with or without the additives. The addition of the oil was made under high-speed homogenization using a high-speed homogenizer (X1000D Unidrive, Ingenieurbüro CAT, Ballrechten-Dottingen, Germany) with a 10 mm diameter generator, a 4eflon bearing, an immersion depth of 150 mm, and at 10,000 rpm. Following the complete addition of the oil, the homogenization was carried on for 3 more minutes at 20,000 rpm [41]. Afterwards, emulsions were allowed to reach a steady state for a few hours before any further experiments or observations were made. Due to the drop sizes and the density mismatch between oil (density equal to 0.916 g/cm³) and water, the systems were then separated into two layers, namely a serum and cream layer. The cream layer (emulsion) was used for all further analysis as well as for the stability assessment. Creaming is a natural phenomenon that is reversible under stirring. Coalescence is an irreversible phenomenon that leads to a macroscopic oil layer that is visible on the top of the emulsion. In the following sections, we will distinguish the two phenomena and discuss stability against creaming or coalescence.

2.3.2. Droplet Dimension Determination by Static Light Scattering (SLS)

A Mastersizer 2000 granulometer (Malvern Instruments Ltd., Malvern, UK) and the Mie theory were used to measure the emulsions' droplet size. Samples were added to

the “small volume sample dispersion unit” after proper dilution. The size distribution was characterized in terms of the surface-averaged diameter D and polydispersity P . The polydispersity index, also called uniformity (U), is defined as the volume-average difference between the diameter and the median diameter, normalized by the median diameter. The median diameter corresponds to the midpoint of the size distribution, meaning the diameter for which half of the dispersed phase is distributed in drops smaller than the median diameter and the other half is distributed in drops larger than the median diameter. These values result from Equations (1) and (2), where N_i is the total number of droplets with diameter D_i and D_{50} is the median diameter, i.e., the diameter for which the cumulative undersized volume fraction is equal to 50% [42,43].

$$D = \frac{\sum_i N_i D_i^3}{\sum_i N_i D_i^2} \quad (1)$$

$$P = \frac{1}{D_{50}} \frac{\sum_i N_i D_i^3 |D_{50} - D_i|}{\sum_i N_i D_i^3} \quad (2)$$

2.3.3. Droplet Morphology Observation by Cryogenic Scanning Electron Microscopy (Cryo-SEM) and Microscopic Observation

A Leica DM IRB (Leica Microsystems GmbH, Wetzlar, Germany) inverted research microscope was used for the emulsion droplet observation. The microscope was equipped with $\times 4$, $\times 10$, $\times 20$, $\times 40$, and $\times 63$ lenses. Samples were diluted using distilled water at the appropriate pH for each sample, specifically pH 7 for SPI samples and pH 3 for PPI samples. Samples were then placed on a microscope slide without a cover, and they were observed in a bright field.

Cryo-SEM observations were carried out with a ZEISS GEMINI 300 field emission scanning electron microscope operating at 1.5 kV. This SEM is equipped with a cryo stage PP3010T from Quorum Technologies, England. A small amount of emulsion was first set on the specimen holder and then frozen in a slushy nitrogen freezing station. Rapid freezing reduces ice crystal damage and results in improved specimen preservation. The sample was transferred into the cryo preparation chamber, held at -140 °C, and fractured with a cold blade. Then it was etched at -90 °C for 3 min or directly coated with platinum. Finally, the sample was inserted onto a highly stable SEM cold stage for observation [44].

It is worth noting that FFTEM and cryo-SEM differ in two major aspects. In FFTEM, after freeze fracturing, a replica of the sample is observed by TEM, while in cryo-SEM, after freeze fracturing, it is the sample itself that is observed by SEM and not by TEM.

2.4. Assessment of the Emulsions' Stability against Creaming

2.4.1. Determination of the Creaming Index Percentage (CI%)

To assess the stability of the emulsions against creaming, storage tests in two conditions were performed. In one case, emulsions (empty and loaded) were prepared in 12 mL flat bottom glass tubes (15 mm in diameter and 50 mm in height) with screw caps and were kept at ambient temperature. In the second case, the vials were kept in the fridge at 4 °C. The systems were separated into two layers (cream/emulsion and serum), within a few minutes after they were prepared. The formation and proportion of the cream layer (emulsion) during storage were observed. The data were collected every 5 days. Their stability against creaming was quantified by the creaming index (CI%), which represents the cream layer height (H_c) expressed as a percentage of the total height of the emulsion height (H_E) in the tube and is calculated by Formula (3) [45]. The procedure was carried out three times.

$$CI = \left(\frac{H_c}{H_t} \right) \times 100(\%) \quad (3)$$

2.4.2. Determination of the Percentage of Adsorbed Proteins (AP%)

The bicinchoninic acid (BCA) method was also employed in order to determine the percentage of adsorbed proteins (AP%) as a means of explanation for each emulsion's stability time. The BCA assay method is based on the fact that the sodium salt of bicinchoninic acid reacts with the cuprous ion generated by the biuret reaction under alkaline conditions. The bicinchoninic acid cuprous complex forms a deep blue color that is read at 562 nm, and the detection range is 0.2–50 µg [46]. For this procedure, 1 mL of the pH-treated SPI and PPI particle dispersions, as well as 1 mL of the serum phase of the emulsion, were centrifuged (10,000 × g, 5 min). The protein content of the supernatants was measured by the bicinchoninic acid (BCA) assay [47]. The protein fraction (AP%) was calculated by Equation (4), in order to assess the amount of proteins that are adsorbed on the oil-water interface.

$$AP = \left[\frac{C_0 - C_s}{C_0} \right] \times 100(\%) \quad (4)$$

In the formula, C_0 was the protein concentration in the initial dispersions, and C_s was the protein concentration in the aqueous phase [48]. The absorbance measurements were performed with a Safire2 (Tecan, Männedorf, Switzerland) plate reader. The procedure was carried out three times.

2.5. Assessment of the Emulsions' Antioxidant Capacity by DPPH Free Radical or ABTS + Cation Scavenging

The emulsions' antioxidant capacity was measured by a colorimetric DPPH assay. The procedure followed was the one previously described by Bi et al., (2021) [49] with slight modifications. Briefly, 2 mL of a DPPH solution in ethyl acetate (0.108 mM) was measured in a plastic tube, and afterwards, 100 µL of sample was added. The mixture was vigorously shaken and kept in the dark for 30 min. Following that, the absorption was measured at 515 nm. Ethyl acetate was used as a blank and a mixture of 2 mL DPPH and 100 µL of ethyl acetate was used as the control sample. The % inhibition of the free radical was calculated with Formula (5), where A_0 is the control sample's absorption and A_1 is the absorption after the 30 min reaction time [49].

The ABTS assay was also employed as a means to verify the scavenging ability of the bioactives against free radicals. The total antioxidant activity is measured by the ABTS + radical cation decolorization assay involving a preformed ABTS ÷ radical cation. ABTS ÷ is prepared by reacting ABTS (7 mM) with potassium persulfate (140 mM) in a ratio of 1:0.5, and the mixture is allowed to stand in the dark at room temperature for 16 h before use. The radical cation is stable in this form for more than 2 days in storage in the dark at room temperature. Prior to assay, the solution is diluted in water to give an absorbance at 734 nm of 0.70 ± 0.02. The ratio of radical to sample was 1:20. Formula (5) was also used in this case in order to deduce the samples' antioxidant activity. The absorbance was measured for the ABTS at 734 nm before the addition of the samples. After the addition of the samples, the absorbance was measured again after 30 min [50].

$$\%Inhibition = \left[\frac{A_0 - A_1}{A_0} \right] \times 100(\%) \quad (5)$$

3. Results and Discussion

In the present study, two O/W emulsions stabilized by PPI or SPI particles were prepared, and α-tocopherol or squalene were encapsulated in the oil droplets. The PPI and SPI particles were produced from native PPI and SPI, respectively, via the pH shifting method. The emulsions were prepared by high-speed homogenization. The particles shape was assessed by FFTEM, and their size was measured with the use of DLS, while the emulsions were macroscopically observed to assess their stability against creaming with the aid of the creaming index and against coalescence. Their morphology was evaluated microscopically with an optical microscope, and their size was measured with the use of a

Mastersizer granulometer. The antioxidant capacity of both empty and loaded emulsions was evaluated by a DPPH colorimetric assay.

3.1. Particles' Preparation, Dimensional Determination, and Morphology Observation

The preparation of both SPI and PPI particles has been studied before with time and pH conditions to optimize the particles' preparation methods [51–54]. The proper modification of the particles is of great importance, as the stability, type (O/W or W/O), and morphology of particle emulsions are highly dependent on the properties of solid particles [55]. Liang & Tang (2014) found that at pH 3.0, most of the proteins in PPI were in the nanoparticle form [37]. For SPI particles, Jiang et al. suggested that the best method to obtain nanoparticles is the one described at Section 2.2, after treating SPI at several pH values and different treatment times, having found that pH 3.0 is the optimum for SPI [38]. In order to quantify the amount of protein converted to particles, the following test was performed: After the preparation of particles at 0.3% *w/w*, a measured volume was placed in a centrifuge tube. The content of the tube was centrifuged at $8500 \times g$ for 20 min in order to collect the particles. Afterwards, the supernatant, which contained the dissolved proteins that had not converted to particles, was collected in a pre-weighed container. The water was removed by freeze-drying, and the container was weighed again. The difference in weight was converted into a percentage, and the results for PPI were that 77% of the protein is converted, compared to 67% of the SPI proteins.

Dynamic light scattering was applied in order to measure the size of the particles after their acidic treatment. All dispersions exhibited a wide and heterogeneous particle size distribution profile, with sizes ranging from 128–255 nm for the PPI particles and from 26–422 nm for the SPI particles. The fact that the particles are not monodispersed is also mirrored in the PDI values. These results are in accordance with those of previous studies [37,56]. PPI and SPI dispersions were also measured by DLS prior to pH treatment for comparative purposes. Both protein isolates had two major size groups. For PPI the 2 size populations were at 1041 nm (79.5% Intensity) and at 109.4 nm (20.5% Intensity), while for SPI at 1259 nm (70.1% Intensity) and 190.5 nm (29.9% Intensity) [57]. Furthermore, DLS was used to determine the ζ -potential of the particles. It was found that for SPI the ζ -potential was -31.37 ± 0.67 mV, and for PPI it was $+32.77 \pm 0.32$ mV. ζ -potential for both those particles has been measured before. The results presented are in accordance with those previously published [53,58].

FFTEM images were also obtained and proved that the particles are of spherical shape, thus the DLS's hypothesis of spherical objects can be applied without misrepresenting the obtained results. The main goal of the FFTEM was indeed to assess particle morphology. We chose not to exploit this technique to deduce particle sizes because many artefacts could alter this determination (dilution, filtration, the position of the fracture that may not capture the equatorial position, etc.). Nevertheless, this method was preferred to TEM, which would have required a drying process that could have altered the particle morphology. Instead, the sizes were determined by DLS. In Figure 1, FFTEM images of PPI particles (A) and SPI (B) are presented. The images provided are of the main size population of each protein. As can be seen in Table 1, most of the PPI particles' diameter was around 128 nm, while for SPI particles it was mainly about 26 nm. Images of protein particles have been obtained before with the freeze-fracture technique and are in accordance with the ones obtained for this project [59].

Table 1. Dynamic light scattering results of the particles' hydrodynamic diameters and PDI. Each value in the table is represented as the mean \pm SD (n = 3).

	Peak 1 (nm)	Peak 2 (nm)	Peak 3 (nm)	PDI
PPI particles	128 \pm 57	293 \pm 50	555 \pm 50	0.494 \pm 0.049
SPI particles	26 \pm 3	270 \pm 43	422 \pm 32	0.404 \pm 0.099

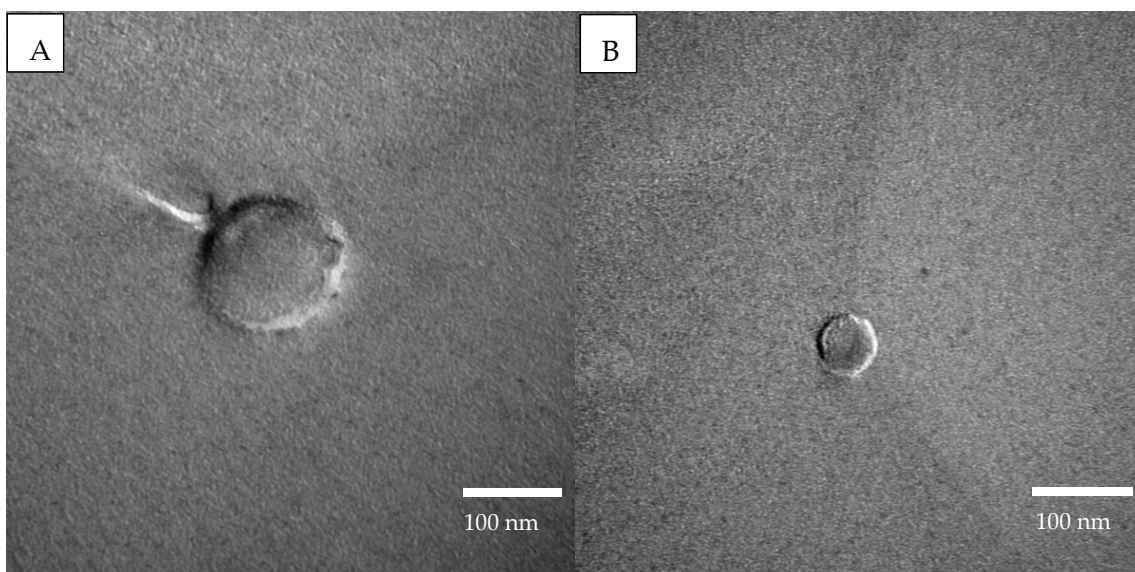


Figure 1. FFTEM images at 75.0 kV of (A) PPI particles (150,000 \times magnification) and (B) SPI particles (200,000 \times magnification).

3.2. Emulsions' Preparation, Droplets Dimensional Determination, and Morphology Observation

In order to form emulsions with the best possible characteristics, such as stability against coalescence, droplet dimensions, and antioxidant ability, several factors have to be considered. Such parameters are the concentration of particles, the oil type, and its volume fraction, as well as the homogenization method. These parameters are the most important factors for emulsion stability and droplet size [60]. For this purpose, several combinations of particle concentrations and water:oil ratios were tested. Furthermore, different homogenization speeds and homogenization times were applied. One more parameter that was tested was the type of oil that was used. Both particles (PPI and SPI) were used at four different concentrations, namely 0.1, 0.2, 0.3, and 0.5% *w/v*. All concentrations were tested in 80:20, 70:30, and 60:40 water: oil ratios. The homogenization times that were tested were 1, 2, and 3 min. Homogenization speeds ranged from 5000 to 20,000 rpm. For the oil phase EVOO, sunflower oil and MCT oil were examined. With these combinations, the one with 0.3% *w/v* particles and 70:30 water: oil ratio was considered the best in terms of stability and incorporation capability, as all of the oil was able to be encapsulated, and the droplet size that was acquired was the smallest. EVOO was chosen as the oil phase since sunflower oil and MCT oil could not be fully incorporated into the emulsion at the 70:30 water:oil ratio. In pursuit of an explanation, control emulsions of oil and water (with no particles) were prepared under the same conditions as the emulsions. It was observed that EVOO formed emulsions that remained stable for several days, while the emulsions formed by sunflower oil or MCT collapsed after 2 days. This could be due to the fact that EVOO is a mixture of triglycerides of several fatty acids and small quantities of other components that display surface-active abilities [61–64]. This means that EVOO may also exhibit emulsifying/stabilizing properties or components able to promote particle adsorption; thus, it was chosen as the most promising candidate for the present study. Nevertheless, the emulsions were observed at times larger than the control destabilization time to ensure that they were also stabilized by the Pickering effect. Hence, all systems that were used to encapsulate the bioactive compounds and that were further analyzed had a 0.3% *w/v* particle concentration and a 70:30 water:EVOO ratio with both protein isolates.

3.2.1. Droplet Size Determination by Static Light Scattering (SLS)

SLS uses the technique of laser diffraction to measure the particle size and particle size distribution of materials. It does so by measuring the intensity of light scattered as a laser

beam passes through a dispersed sample. This data is then analyzed to calculate the size of the particles that created the scattering pattern.

In Table 2, the droplet size of empty and loaded emulsions is presented. All samples show a uniformity ranging from 0.3 to 0.45, showing that the emulsions are quite polydisperse; nevertheless, the distributions remain monomodal. In addition, a representation of the PPI empty sample's droplet diameter distribution is given as an example in Figure 2. This came as no surprise since the particles that stabilized them were very heterogeneous in terms of size and therefore led to droplets of various sizes. Several studies have examined the fact that particles' size affects the emulsions' droplet diameter in a proportional manner, meaning that bigger particles form larger droplets [65–67] in the case where particles are in excess in the continuous phase. The two kinds of emulsions seem to have similar droplet sizes, since the difference in diameter is not significant when taking into account the polydispersity of the emulsions. This is also supported by the fact that the particles that stabilize these emulsions do not differ much, in terms of size, as shown in Table 1. Another useful conclusion that could be drawn from the measurements is that the encapsulation of both α -tocopherol and squalene does not have an effect on the droplet size. Previous studies have also reported that no size differences were observed after the encapsulation of bioactive compounds [68]. This indicates that the two molecules are likely encapsulated in the core of the drops and do not perturb the interface.

Table 2. Determination of the emulsions' droplet diameter and uniformity by static light scattering. Each value in the table is represented as mean \pm SD ($n = 3$). A t -test was employed for the statistical analysis. Significant differences between values in the same column are indicated by different letters a, and b ($p < 0.1$).

Sample	d (μm)	Uniformity
PPI empty	57.9 ^a \pm 0.1	0.30 ^a \pm 0.01
PPI α - tocopherol	57.0 ^a \pm 0.1	0.31 ^a \pm 0.01
PPI squalene	62.2 ^b \pm 0.5	0.31 ^a \pm 0.01
SPI empty	60.0 ^a \pm 6.9	0.45 ^a \pm 0.03
SPI α - tocopherol	66.4 ^a \pm 1.5	0.38 ^b \pm 0.01
SPI squalene	67.7 ^a \pm 5.0	0.41 ^a \pm 0.02

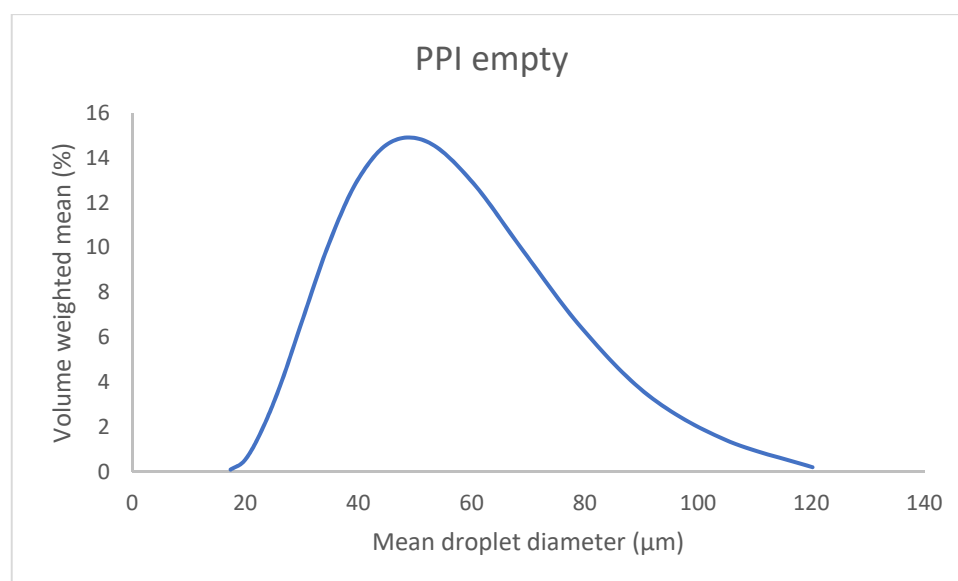


Figure 2. Mean droplet diameter of the PPI empty emulsion obtained by static light scattering.

3.2.2. Droplet Morphology Observations by Cryogenic Scanning Electron Microscopy (Cryo-SEM) and Microscopic Observation

The emulsions' droplets were observed by cryo-SEM and an optical microscope. The images obtained from the microscope showed spherical droplets with various sizes, which supports the large value of the uniformity obtained from the SLS measurements. Such images have been observed in previous works that have focused on the preparation of O/W emulsions stabilized by pea and soy protein isolates [58,69–71]. The texture of the droplets can also be commented on, since in some images, droplets appear to have a smooth surface (Figure 3A), while in others, there seems to be a rough layer (Figure 3B) around them of probably larger particles or insoluble proteins. Those smaller droplets during the SLS measurements were probably “hidden” from the dominant larger ones. When droplet size was measured manually from the microscopy images, the resulting size was slightly smaller than that obtained with the Mastersizer.

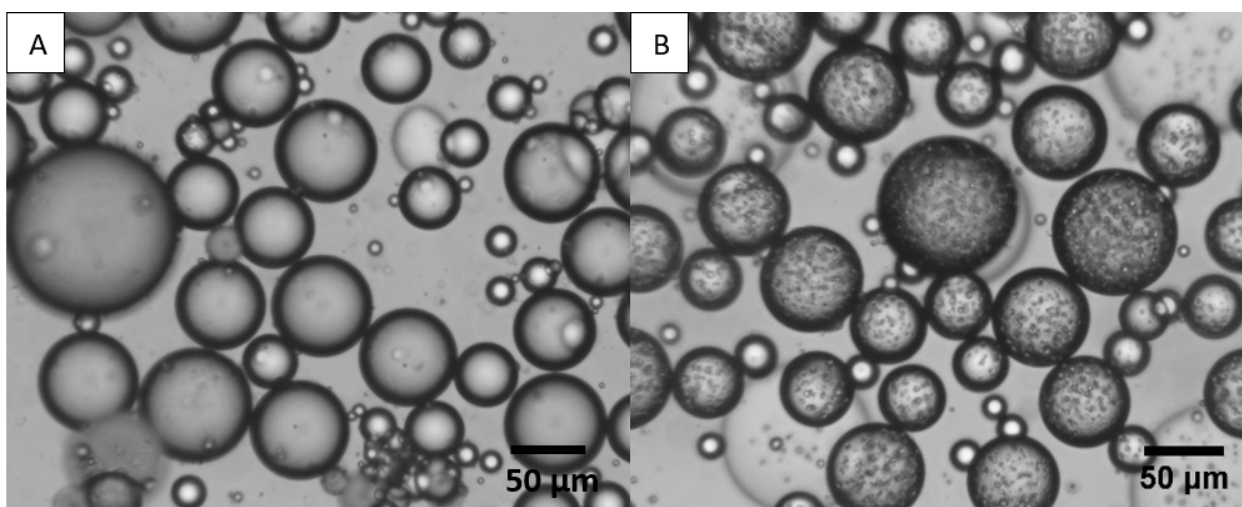


Figure 3. A $\times 10$ magnification of PPI empty emulsions of (A) droplets with a smooth surface, and (B) droplets with a rough surface. The two images were taken from the same emulsion.

On the other hand, cryo-SEM analysis made it quite difficult to provide a distinct outline of individual particles at the interface of droplets. It was also challenging to make the observations, especially at high magnification, because samples were thermally sensitive and the radiation from the electron beam led to melting. Such a phenomenon can be seen in Figure 4A, where cracks are visible. It sometimes seems as though there are two levels of roughness, but it is hard to say because zooming is not possible due to the sensitivity of the samples (Figure 4B). Nevertheless, some concrete results can be collected, such as the round shape of the particles as well as the droplets. In addition, a clear image of a droplet covered by SPI particles is presented in Figure 4C. Furthermore, the data and images that were collected are supported by figures published in other studies [72,73].

3.3. Stability Assessment against Creaming and Coalescence of the Emulsions

The stability of the emulsions against creaming was assessed by monitoring the emulsions' CI% during storage. Two different storage conditions were examined, namely 4 °C and 25 °C. All the emulsions, freshly prepared, underwent a fast creaming process. The emulsions stability was assessed by their respective creaming stability in terms of percentage creaming index (CI%) upon storage. The emulsions' CI% was measured every three days up to the point of collapse. The %CI of the SPI empty as well as the loaded emulsions is 66.7% at day 0 (Figure 5a), while for the PPI it is 53.3% (Figure 5e). If the emulsion occupies 53.3% of the volume while the volume fraction of oil is 31.9% (density of EVOO = 0.916 g.cm⁻³), this means that droplets are packed with a capacity of 0.60 in the PPI-stabilized emulsion, a value close to the random close packing, or, in other words,

drops of cream without strong interactions. The compacity is a bit lower (0.48%) in the SPI-stabilized emulsions, likely due to some weak drop attractions. For the SPI samples that were stored at ambient temperature, the CI% started to decrease gradually, and at 10 days, oil was visible on top of the emulsions and reached 13.3% (Figure 5b) meaning a destabilization through coalescence. On the other hand, PPI emulsions stored at the same conditions were more stable (Figure 5e,f) against both creaming and coalescence. At 10 days, a small quantity of oil was visible on top of the empty emulsion and the one loaded with squalene. CI% remained the same for the α -tocopherol containing emulsion, while it reached 50.1% for the other two PPI emulsions (Figure 5f). Microbial growth was also observed on some of the emulsions after the tenth day of storage at 25 °C. Microbial growth was not observed for samples containing α -tocopherol and squalene that were stored at ambient temperature and for all samples that were stored at 4 °C. It has been previously reported that microbial growth started for SPI emulsions after 6 days of storage at ambient temperature and after 9 or 10 days for PPI emulsions [74,75]. Furthermore, squalene as well as α -tocopherol have been found to act against microorganisms, which explains the resistance of the samples containing them against microbial growth [76,77].

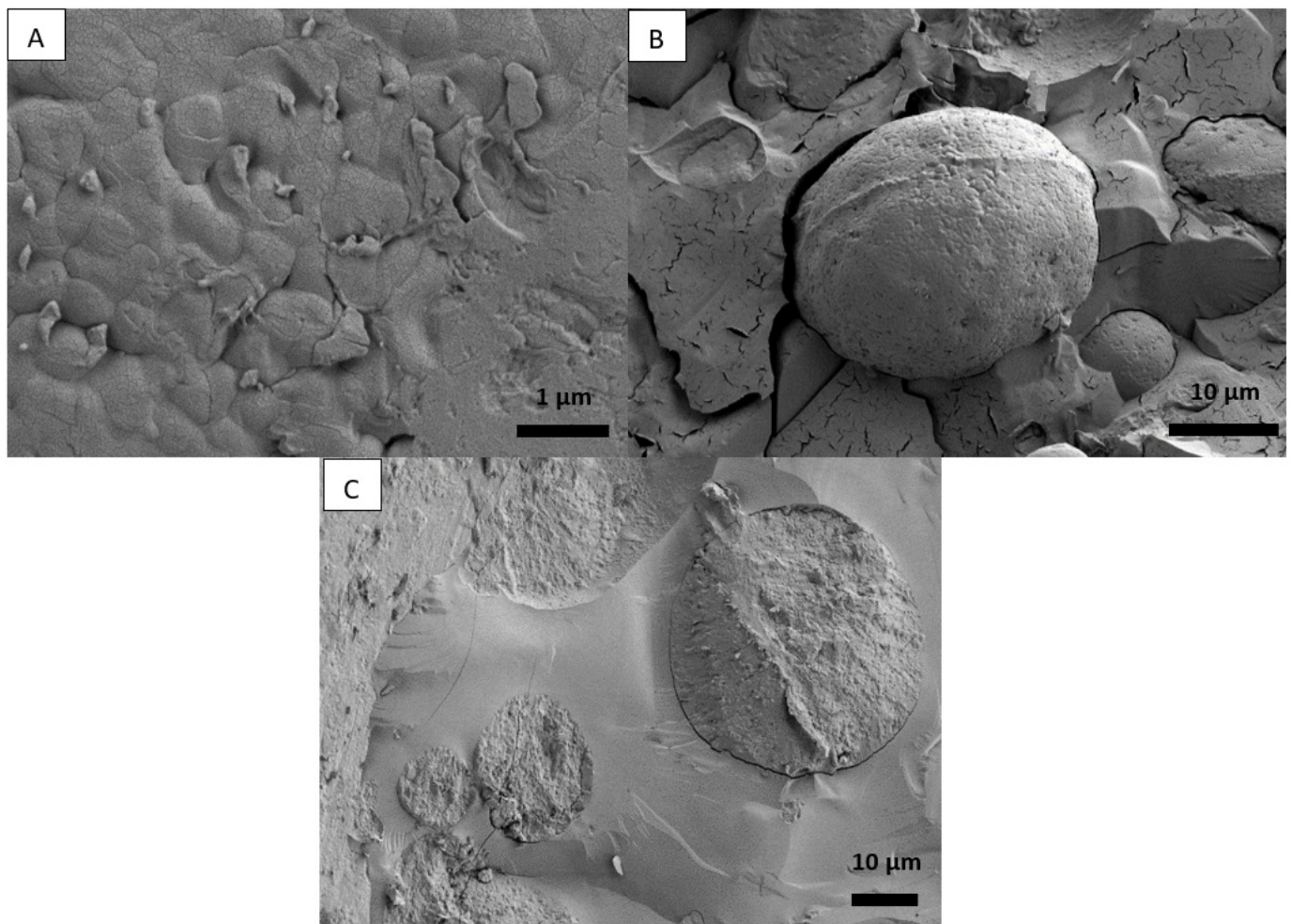


Figure 4. Cryo-SEM image of (A) PPI emulsion, (B) PPI emulsion droplet covered by PPI particles, and (C) SPI emulsion droplets covered by SPI particles.

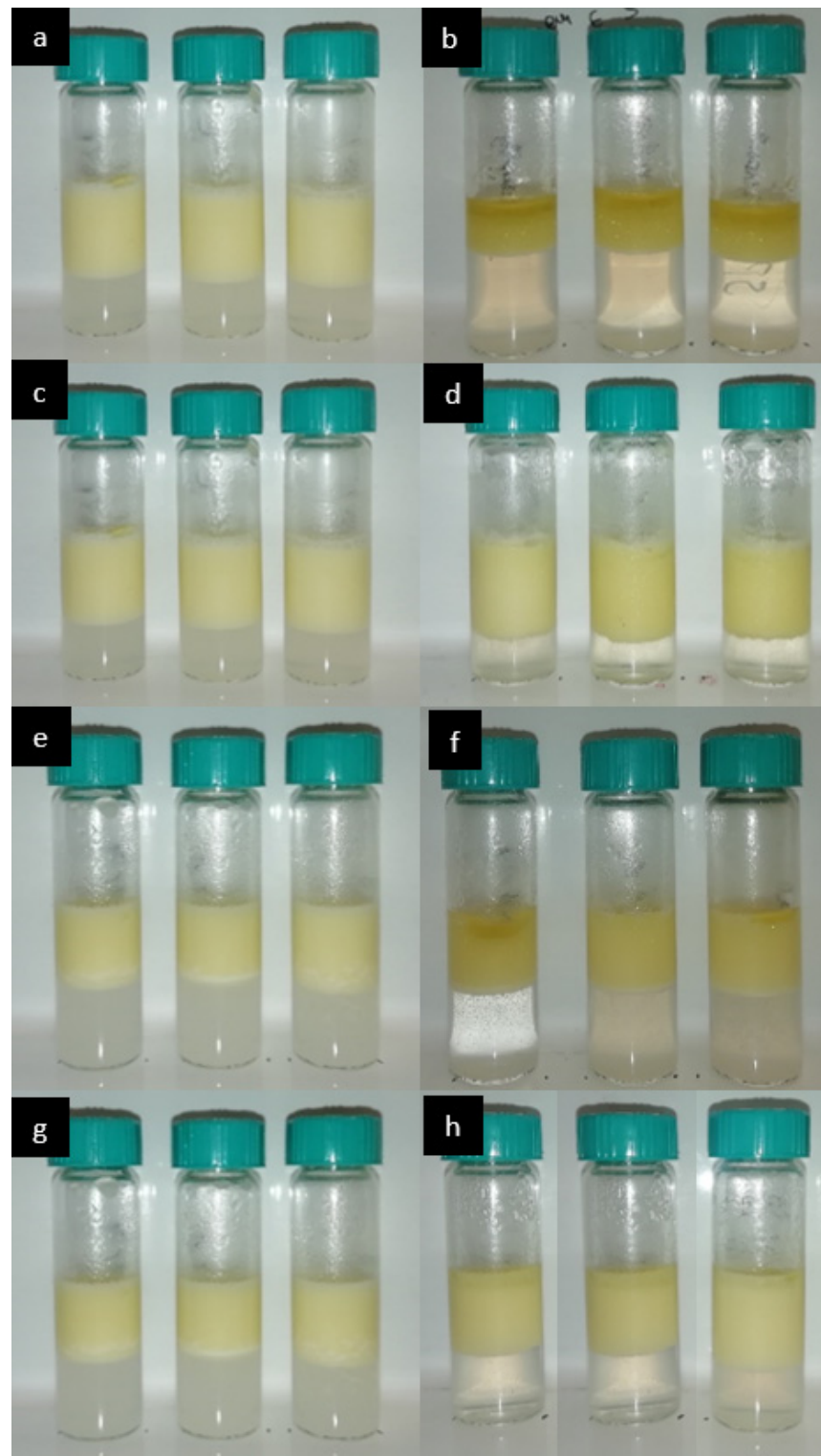


Figure 5. (a) SPI-stabilized emulsions at day 0, 25 °C, from left to right: empty, with α -tocopherol, with squalene, (b) SPI-stabilized emulsions at day 10, 25 °C, from left to right: empty, with α -tocopherol, with squalene, (c) SPI-stabilized emulsions at day 0, 4 °C, and (d) SPI-stabilized emulsions at day 10, 4 °C, from left to right: empty, with α -tocopherol, with squalene, (e) PPI-stabilized emulsions at day 0, 25 °C, from left to right: empty, with α -tocopherol, with squalene, (f) PPI-stabilized emulsions at day 10, 25 °C, from left to right: empty, with α -tocopherol, with squalene, (g) PPI-stabilized emulsions at day 0, 4 °C, and (h) PPI-stabilized emulsions at day 10, 4 °C, from left to right: empty, with α -tocopherol, with squalene.

Storage at 4 °C increased the stability of both types of emulsion. The cream after the first few hours of storage was much firmer, which is expected since EVOO's viscosity at 4 °C is higher than at room temperature [78]. The CI% does not change for any of the samples for a period of more than 60 days (Figure 5), and no oil release is observed for any of the emulsions.

The AP% is also a strong indication of an emulsion's stability against coalescence and creaming, since a higher amount of protein stabilizes the emulsion further, but there is a certain threshold of protein concentration that can be adsorbed at the oil-water interface. In this case, 70% of the initial protein content was adsorbed at the oil-water interface of PPI emulsions, while the adsorption decreased to 45% for the SPI emulsions. This fact explains, in a certain degree, the increased stability of the PPI emulsions against those stabilized by SPI. The higher amount of non-adsorbed SPI may also explain the lower compacity of the creamed emulsion as the non-adsorbed protein can induce attractive interactions through depletion. Previous studies have reported that the AP% for PPI stabilized emulsions, with PPI concentrations up to 1% *w/w*, reached 84.33% [79]. On the other hand, lower AP% values that reach 19.9%, for concentrations under 1% *w/w* have been reported for SPI [80]. The main explanation behind these results lies in the isolates' composition and surface hydrophobicity. The consistency of both SPI and PPI has been previously studied, and it has been found that 80% of the SPI proteins are 7S (b-conglycinin) and 11S (glycinin), which are highly soluble, while convicillin, vicilin, and a- and b- subunits of legumin constitute the most part of the PPI protein fraction [81,82]. The highest hydrophobicity of pea proteins explains their better adsorption at the oil-water interface. PPI is also the only isolate that was found to contain fat, increasing its affinity towards the oil phase of the emulsion [9]. It has also been reported that the surface hydrophobicity of SPI proteins decreases when the SPI treatment happens under 90 °C, affecting its emulsifying capacity [83].

3.4. Assessment of the Emulsions' Antioxidant Capacity by DPPH Free Radical Scavenging

The antioxidant capacity of O/W emulsions was measured spectrophotometrically, with the DPPH and ABTS cation scavenging techniques over time to observe the reaction between the free radicals and the emulsions. Table 3 includes the % scavenging of the DPPH and ABTS cation free radicals 30 min after the addition of the emulsion in the DPPH solution. The 30-min time frame gives the reaction enough time to reach a plateau, so that the scavenging potential measured in each sample would be the maximum.

Table 3. % scavenging ability of empty PPI and SPI emulsions and their respective loaded ones with α -tocopherol or squalene. Each value in the table is represented as the mean \pm SD (n = 3). A t-test was employed for the statistical analysis. Significant differences between values in the same row are indicated by different letters a, b, and c ($p < 0.1$).

% DPPH Scavenging		
PPI empty	PPI α -tocopherol	PPI squalene
37.3 ^a \pm 0.7	86.1 ^c \pm 0.1	62.0 ^b \pm 0.1
SPI empty	SPI α -tocopherol	SPI squalene
39.5 ^a \pm 0.1	83.6 ^c \pm 0.1	60.6 ^b \pm 0.1
% ABTS Scavenging		
PPI empty	PPI α -tocopherol	PPI squalene
26.1 ^a \pm 0.9	77.8 ^c \pm 0.3	52.4 ^b \pm 0.1
SPI empty	SPI α -tocopherol	SPI squalene
25.5 ^a \pm 0.1	68.5 ^c \pm 0.2	58.7 ^b \pm 0.3

The results obtained show that all emulsions have a scavenging effect against both radicals, suggesting that they can be characterized as antioxidants at least for this kind of antioxidant mechanism. Both for the SPI and the PPI emulsions, the empty ones exhibit the lowest antioxidant effect. The difference in the antioxidant effect between the two empty emulsions is not significant, indicating that whatever antioxidant effect appears comes from the EVOO and the protein contribution is minimal, if not nonexistent. EVOO's antioxidant capacity is well-known and widely studied, while for SPI and PPI, antioxidant capacity has been reported when they are previously hydrolyzed [84,85]. Moving on to the loaded emulsions, it is clear in both systems that the ones containing α -tocopherol exhibit higher antioxidant activity than those that contain squalene. Previously published studies that have examined the roles of several molecules, including squalene and α -tocopherol, in lipid environments have shown that α -tocopherol is the dominant antioxidant compound. More specifically, Naziri et al., 2015 studied the contribution of squalene and tocopherols on the oxidative stability of cold-pressed pumpkin seed oil and showed that the antioxidant activity of squalene commenced 3 weeks into the study, while α -tocopherol was the molecule that acted as an antioxidant during that time [86]. Furthermore, studies that examined the degradation rates of squalene, α -tocopherol and phenolics, reported that α -tocopherol had the highest degradation rate because it acted protectively over squalene's and phenols' oxidation. Those studies also suggest, as an explanation of squalene's reduced antioxidant capacity, the competitive oxidation of different lipids present in olive oil [87]. Moreover, antioxidant activity, in general, mainly depends on the number and positions of phenolic hydroxyl groups. This fact stands in favor of α -tocopherol's superior antioxidant ability [88–90]. On the other hand, α -tocopherol has been proven to be a rather effective antioxidant, especially in lipid-based systems, since it can act synergistically with other molecules that exhibit antioxidant activity [91,92]. One more factor that can affect the system's antioxidant ability is the placement of the antioxidants in the oil droplet. Although both compounds are oil soluble, α -tocopherol has the hydroxy-phenol group that could orient the molecule closer to the water-oil interface. One more factor that affects the antioxidant ability of a molecule is the length of the alkyl chain. The antioxidant capacity increases with the increase of the alkyl chain up to a point, and then it starts to decrease. It has been found that the optimum antioxidant activity is achieved with chain lengths from 2 to 13 carbon atoms. From that point of view, the antioxidant activity declines [93]. If we do not take into account the carbon atoms of α -tocopherol's phenol group, which are not in an open chain, then we can see that squalene has a significantly higher number of carbon atoms in an open chain than α -tocopherol. Between the SPI and PPI systems, loaded with either α -tocopherol or squalene, no remarkable difference can be reported.

4. Conclusions

Pea and soy protein isolates were used to create particles via the pH shifting method to form two O/W emulsions. The particles formed were of spherical shape and polydispersed, leading to emulsions with a quite high value of uniformity in terms of droplet size while maintaining a monomodal drop size distribution. These emulsions were then used for the encapsulation of two bioactive compounds, namely α -tocopherol and squalene. Both kinds of emulsions had EVOO as the oil phase. The water:oil ratio that was finally examined was 70:30 *w/w*. Both particles successfully formed emulsions at this ratio. The droplets of the two kinds of emulsions were of similar size and spherical shape. The encapsulation of the bioactives, at least at the concentration used in the present study, did not appear to have a great effect on the size. The stability of the emulsions was tested under two conditions. More specifically, empty and loaded emulsions, were stored at ambient temperature and at 4 °C, and it was found that while at room temperature PPI emulsions were more stable than SPI emulsions, when stored at 4 °C, no big differences in stability were detected. Empty and loaded emulsions exhibited antioxidant activity, with a noticeable increase in antioxidant activity when loaded at 1% of α -tocopherol or squalene. SPI and PPI emulsions loaded

with α -tocopherol exhibited the highest scavenging ability of all other samples against the DPPH free radical and the ABTS cation.

Overall, PPI and SPI were successful in forming particles that stabilized emulsions that were used for the encapsulation of α -tocopherol or squalene. The additives enhance the systems' antioxidant capacity. The use of EVOO as the oil phase provides the system with added nutritional value. The use of proteins as stabilizers, as well as the presence of olive oil and the two bioactive compounds, lead us to believe that these systems are very good candidates as delivery systems of nutraceuticals in foods and especially plant-based products.

Author Contributions: Conceptualization, M.D.C.; methodology, E.G and I.L.; validation, M.D.C. and V.S.; investigation, E.G. and E.L.; resources, A.X.; data curation, E.G.; writing—original draft preparation, E.G. and M.D.C.; writing—review and editing, A.X. and V.S.; supervision, M.D.C.; project administration, A.X.; funding acquisition, A.X. All authors have read and agreed to the published version of the manuscript.

Funding: This research was funded by European Regional Development Fund of the European Union and Greek national funds through the Operational Program Competitiveness, Entrepreneurship, and Innovation, under the call RESEARCH–CREATE–INNOVATE, T2EAK_03640.

Institutional Review Board Statement: Not applicable.

Informed Consent Statement: Not applicable.

Data Availability Statement: Available upon request.

Acknowledgments: A.X. thanks the University of Bordeaux, IdEx, and the visiting scholars for his stay. EG would like to thank the Centre de Recherche Paul Pascal (CRPP) for the accommodations provided to carry out the cryo-SEM, FFTEM, microscopic observations, and droplet size measurement (SLS) experiments. Cryo-SEM was carried out at the Bordeaux Imaging Center by Isabelle Svahn. EG's stay was financed by the European Regional Development Fund of the European Union and Greek national funds through the Operational Program Competitiveness, Entrepreneurship, and Innovation, under the call RESEARCH–CREATE–INNOVATE, T2EAK_03640.

Conflicts of Interest: The authors declare no conflict of interest.

References

1. Deckers, J. Obesity, Public Health, and the Consumption of Animal Products: Ethical Concerns and Political Solutions. *J. Bioeth. Inq.* **2013**, *10*, 29–38. [[CrossRef](#)] [[PubMed](#)]
2. Salter, A.M. Impact of Consumption of Animal Products on Cardiovascular Disease, Diabetes, and Cancer in Developed Countries. *Anim. Front.* **2013**, *3*, 20–27. [[CrossRef](#)]
3. Espinosa, R.; Tago, D.; Treich, N. Infectious Diseases and Meat Production. *Environ. Resour. Econ.* **2020**, *76*, 1019. [[CrossRef](#)]
4. Hölker, S.; von Meyer-Höfer, M.; Spiller, A. Animal Ethics and Eating Animals: Consumer Segmentation Based on Domain-Specific Values. *Sustainability* **2019**, *11*, 3907. [[CrossRef](#)]
5. Willett, W.; Rockström, J.; Loken, B.; Springmann, M.; Lang, T.; Vermeulen, S.; Garnett, T.; Tilman, D.; DeClerck, F.; Wood, A.; et al. Food in the Anthropocene: The EAT–Lancet Commission on Healthy Diets from Sustainable Food Systems. *Lancet* **2019**, *393*, 447–492. [[CrossRef](#)]
6. McClements, D.J. Future Foods: A Manifesto for Research Priorities in Structural Design of Foods. *Food Funct.* **2020**, *11*, 1933–1945. [[CrossRef](#)]
7. Boye, J.I.; Danquah, A.O.; Lam Thang, C.; Zhao, X. Food Allergens. In *Food Biochemistry and Food Processing*, 2nd ed.; John Wiley & Sons, Inc.: Hoboken, NJ, USA, 2012; Chapter 42; pp. 798–819. [[CrossRef](#)]
8. Barac, M.B.; Pesic, M.B.; Stanojevic, S.P.; Kostic, A.Z.; Bivolarevic, V. Comparative Study of the Functional Properties of Three Legume Seed Isolates: Adzuki, Pea and Soy Bean. *J. Food Sci. Technol.* **2015**, *52*, 2779–2787. [[CrossRef](#)] [[PubMed](#)]
9. Zhao, H.; Shen, C.; Wu, Z.; Zhang, Z.; Xu, C. Comparison of Wheat, Soybean, Rice, and Pea Protein Properties for Effective Applications in Food Products. *J. Food Biochem.* **2020**, *44*, e13157. [[CrossRef](#)]
10. Kurek, M.A.; Onopiuk, A.; Pogorzelska-nowicka, E.; Szpicer, A.; Zalewska, M.; Półtorak, A. Novel Protein Sources for Applications in Meat-Alternative Products — Insight and Challenges. *Foods* **2022**, *11*, 957. [[CrossRef](#)] [[PubMed](#)]
11. McClements, D.J. Development of Next-Generation Nutritionally Fortified Plant-Based Milk Substitutes: Structural Design Principles. *Foods* **2020**, *9*, 421. [[CrossRef](#)]
12. Pickering, S.U. CXCVI—Emulsions. *J. Chem. Soc. Trans.* **1907**, *91*, 2001–2021. [[CrossRef](#)]
13. Ramsden, W. Separation of Solids in the Surface-Layers of Solutions and 'Suspensions' (Observations on Surface-Membranes, Bubbles, Emulsions, and Mechanical Coagulation)—Preliminary Account. *Proc. R. Soc. Lond.* **1904**, *72*, 156–164. [[CrossRef](#)]

14. Tavernier, I.; Wijaya, W.; van der Meeren, P.; Dewettinck, K.; Patel, A.R. Food-Grade Particles for Emulsion Stabilization. *Trends Food Sci. Technol.* **2016**, *50*, 159–174. [CrossRef]
15. Horozov, T.S.; Binks, B.P. Particle-Stabilized Emulsions: A Bilayer or a Bridging Monolayer? *Angew. Chem.* **2006**, *118*, 787–790. [CrossRef]
16. Giermanska-Kahn, J.; Laine, V.; Arditty, S.; Schmitt, V.; Leal-Calderon, F. Particle-Stabilized Emulsions Comprised of Solid Droplets. *Langmuir* **2005**, *21*, 4316–4323. [CrossRef]
17. Drusch, S.; Klost, M.; Kieserling, H. Current Knowledge on the Interfacial Behaviour Limits Our Understanding of Plant Protein Functionality in Emulsions. *Curr. Opin. Colloid Interface Sci.* **2021**, *56*, 101503. [CrossRef]
18. Gomes, A.; Sobral, P.J.D.A. Plant Protein-Based Delivery Systems: An Emerging Approach for Increasing the Efficacy of Lipophilic Bioactive Compounds. *Molecules* **2022**, *27*, 60. [CrossRef]
19. Ribeiro, A.M.; Estevinho, B.N.; Rocha, F. The Progress and Application of Vitamin E Encapsulation—A Review. *Food Hydrocoll.* **2021**, *121*, 106998. [CrossRef]
20. Chen, C.C.; Wagner, G. Vitamin E Nanoparticle for Beverage Applications. *Chem. Eng. Res. Des.* **2004**, *82*, 1432–1437. [CrossRef]
21. Thiele, J.J.; Hsieh, S.N.; Ekanayake-Mudiyanselage, S. Vitamin E: Critical Review of Its Current Use in Cosmetic and Clinical Dermatology. *Dermatol. Surg.* **2005**, *31*, 805–813. [CrossRef]
22. Lehman, R.W. Assay of Vitamin E in Pharmaceutical Products. *J. Pharm. Sci.* **1964**, *53*, 201–204. [CrossRef] [PubMed]
23. Vitamin E—Health Professional Fact Sheet. Available online: <https://ods.od.nih.gov/factsheets/VitaminE-HealthProfessional/> (accessed on 9 November 2022).
24. Khanna, S.; Roy, S.; Slivka, A.; Craft, T.K.S.; Chaki, S.; Rink, C.; Notestine, M.A.; DeVries, A.C.; Parinandi, N.L.; Sen, C.K. Neuroprotective Properties of the Natural Vitamin E α -Tocotrienol. *Stroke* **2005**, *36*, 2258–2264. [CrossRef]
25. Nesaretnam, K.; Wong, W.Y.; Wahid, M.B. Tocotrienols and Cancer: Beyond Antioxidant Activity. *Eur. J. Lipid Sci. Technol.* **2007**, *109*, 445–452. [CrossRef]
26. Tan, B.; Watson, R.R.; Preedy, V.R. (Eds.) *Tocotrienols: Vitamin E Beyond Tocopherols*, 2nd ed.; CRC Press: Boca Raton, FL, USA, 2012; Chapter 4. [CrossRef]
27. Tappel, A.L. Vitamin E as the Biological Lipid Antioxidant. *Vitam. Horm.* **1962**, *20*, 493–510. [CrossRef]
28. McCarthy, T.L.; Kerry, J.P.; Kerry, J.F.; Lynch, P.B.; Buckley, D.J. Evaluation of the Antioxidant Potential of Natural Food/Plant Extracts as Compared with Synthetic Antioxidants and Vitamin E in Raw and Cooked Pork Patties. *Meat Sci.* **2001**, *58*, 45–52. [CrossRef]
29. Fox, C.B. Squalene Emulsions for Parenteral Vaccine and Drug Delivery. *Molecules* **2009**, *14*, 3286–3312. [CrossRef]
30. Huang, Z.R.; Lin, Y.K.; Fang, J.Y. Biological and Pharmacological Activities of Squalene and Related Compounds: Potential Uses in Cosmetic Dermatology. *Molecules* **2009**, *14*, 540–554. [CrossRef] [PubMed]
31. Shimizu, N.; Ito, J.; Kato, S.; Otoki, Y.; Goto, M.; Eitsuka, T.; Miyazawa, T.; Nakagawa, K. Oxidation of Squalene by Singlet Oxygen and Free Radicals Results in Different Compositions of Squalene Monohydroperoxide Isomers. *Sci. Rep.* **2018**, *8*, 9116. [CrossRef]
32. Newmark, H.L. Squalene, olive oil, and cancer risk. Review and hypothesis. *Ann. N. Y. Acad. Sci. J.* **1999**, *889*, 193–203. [CrossRef] [PubMed]
33. Owen, R.W.; Mier, W.; Giacosa, A.; Hull, W.E.; Spiegelhalder, B.; Bartsch, H. Phenolic compounds and squalene in olive oils: The concentration and antioxidant potential of total phenols, simple phenols, secoiridoids, lignans and squalene. *Food Chem. Toxicol.* **2000**, *38*, 647–659. [CrossRef]
34. Rao, C.V.; Newmark, H.L.; Reddy, B.S. Chemopreventive effect of squalene on colon cancer. *Carcinogenesis* **1998**, *19*, 287–290. [CrossRef] [PubMed]
35. Cho, S.; Choi, C.W.; Lee, D.H.; Won, C.H.; Kim, S.M.; Lee, S.; Lee, M.J.; Chung, J.H. High-Dose Squalene Ingestion Increases Type I Procollagen and Decreases Ultraviolet-Induced DNA Damage in Human Skin in Vivo but Is Associated with Transient Adverse Effects. *Clin. Exp. Dermatol.* **2009**, *34*, 500–508. [CrossRef]
36. Smith, T.J. Squalene: Potential Chemopreventive Agent. *Expert Opin. Investig. Drugs* **2000**, *9*, 1841–1848. [CrossRef] [PubMed]
37. Liang, H.N.; Tang, C.-h. Pea Protein Exhibits a Novel Pickering Stabilization for Oil-in-Water Emulsions at PH 3.0. *LWT-Food Sci. Tech.* **2014**, *58*, 463–469. [CrossRef]
38. Jiang, J.; Chen, J.; Xiong, Y.L. Structural and Emulsifying Properties of Soy Protein Isolate Subjected to Acid and Alkaline PH-Shifting Processes. *J. Agric. Food Chem.* **2009**, *57*, 7576–7583. [CrossRef]
39. Demisli, S.; Mitsou, E.; Pletsas, V.; Xenakis, A.; Papadimitriou, V. Development and Study of Nanoemulsions and Nanoemulsion-based Hydrogels for the Encapsulation of Lipophilic Compounds. *Nanomaterials* **2020**, *10*, 1–19. [CrossRef] [PubMed]
40. Sharma, K.P.; Kumaraswamy, G.; Ly, I.; Olivier, M.M. Self-Assembly of Silica Particles in a Nonionic Surfactant Hexagonal Mesophase. *J. Phys. Chem. B* **2009**, *113*, 3423–3430. [CrossRef]
41. Mwangi, W.W.; Ho, K.W.; Tey, B.T.; Chan, E.S. Effects of Environmental Factors on the Physical Stability of Pickering-Emulsions Stabilized by Chitosan Particles. *Food Hydrocoll.* **2016**, *60*, 543–550. [CrossRef]
42. Gautier, F.; Destribats, M.; Perrier-Cornet, R.; Dechézelles, J.-F.; Giermanska, J.; Héroguez, V.; Schmitt, V. Pickering Emulsions with Stimulable Particles: From Highly- to Weakly-Covered Interfaces. *Phys. Chem. Chem. Phys.* **2007**, *9*, 6285–6488. [CrossRef]
43. Stasse, M.; Ribaut, T.; Héroguez, V.; Schmitt, V. Elaboration of Double Emulsion-Based Polymeric Capsules for Fragrance. *Colloid Polym. Sci.* **2021**, *299*, 179–191. [CrossRef]

44. Destribats, M.; Lapeyre, V.; Wolfs, M.; Sellier, E.; Leal-Calderon, F.; Ravaine, V.; Schmitt, V. Soft Microgels as Pickering Emulsion Stabilisers: Role of Particle Deformability. *Soft Matter* **2011**, *7*, 7689–7698. [[CrossRef](#)]
45. Firebaugh, J.D.; Daubert, C.R. Emulsifying and Foaming Properties of a Derivatized Whey Protein Ingredient. *Int. J. Food Prop.* **2005**, *8*, 243–253. [[CrossRef](#)]
46. Shen, C.-H. Quantification and Analysis of Proteins. In *Diagnostic Molecular Biology*; Elsevier Inc.: Amsterdam, The Netherlands, 2019; Chapter 8; pp. 187–214. [[CrossRef](#)]
47. Smith, P.K.; Krohn, R.I.; Hermanson, G.T.; Mallia, A.K.; Gartner, F.H.; Provenzano, M.D.; Fujimoto, E.K.; Goeke, N.M.; Olson, B.J.; Klenk, D.C. Measurement of Protein Using Bicinchoninic Acid. *Anal. Biochem.* **1985**, *150*, 76–85. [[CrossRef](#)]
48. Chen, M.; Lu, J.; Liu, F.; Nsor-Atindana, J.; Xu, F.; Goff, H.D.; Ma, J.; Zhong, F. Study on the Emulsifying Stability and Interfacial Adsorption of Pea Proteins. *Food Hydrocoll.* **2019**, *88*, 247–255. [[CrossRef](#)]
49. Bi, W.; Liyuan, G.; Wenjuan, W.; Qiang, X. Skin Targeting of Resveratrol-Loaded Starch-Based Pickering Emulsions: Preparation, Characterization, and Evaluation. *Colloid Polym. Sci.* **2021**, *299*, 1383–1395. [[CrossRef](#)]
50. Pellegrini, N.; Yang, R.M.; Rice-Evans, C. Screening of Dietary Carotenoids and Carotenoid-Rich Fruit Extracts for Antioxidant Activities Applying 2,2'-azinobis (3-ethylenebenzothiazoline-6-sulfonic acid) Radical Cation Decolorization Assay. *Methods Enzymol.* **1999**, *299*, 379–384. [[CrossRef](#)]
51. Tang, C.H. Emulsifying Properties of Soy Proteins: A Critical Review with Emphasis on the Role of Conformational Flexibility. *Crit. Rev. Food Sci. Nutr.* **2017**, *57*, 2636–2679. [[CrossRef](#)]
52. Liu, F.; Tang, C.H. Soy Protein Nanoparticle Aggregates as Pickering Stabilizers for Oil-in-Water Emulsions. *J. Agric. Food Chem.* **2013**, *61*, 8888–8898. [[CrossRef](#)] [[PubMed](#)]
53. Sridharan, S.; Meinders, M.B.J.; Bitter, J.H.; Nikiforidis, C.V. On the Emulsifying Properties of Self-Assembled Pea Protein Particles. *Langmuir* **2020**, *36*, 12221–12229. [[CrossRef](#)] [[PubMed](#)]
54. Niroula, A.; Alshamsi, R.; Sobti, B.; Nazir, A. Optimization of Pea Protein Isolate-Stabilized Oil-in-Water Ultra-Nanoemulsions by Response Surface Methodology and the Effect of Electrolytes on Optimized Nanoemulsions. *Colloids Interfaces* **2022**, *6*, 47. [[CrossRef](#)]
55. Yang, Y.; Fang, Z.; Chen, X.; Zhang, W.; Xie, Y.; Chen, Y.; Liu, Z.; Yuan, W. An Overview of Pickering Emulsions: Solid-Particle Materials, Classification, Morphology, and Applications. *Front. Pharmacol.* **2017**, *8*, 287. [[CrossRef](#)]
56. Yang, Y.; He, S.; Ye, Y.; Cao, X.; Liu, H.; Wu, Z.; Yue, J.; Sun, H. Enhanced Hydrophobicity of Soybean Protein Isolate by Low-PH Shifting Treatment for the Sub-Micron Gel Particles Preparation. *Ind. Crops Prod.* **2020**, *151*, 112475. [[CrossRef](#)]
57. Jiang, S.; Ding, J.; Andrade, J.; Rababah, T.M.; Almajwal, A.; Abulmeaty, M.M.; Feng, H. Modifying the Physicochemical Properties of Pea Protein by PH-Shifting and Ultrasound Combined Treatments. *Ultrason. Sonochem.* **2017**, *38*, 835–842. [[CrossRef](#)] [[PubMed](#)]
58. Chen, W.S.; Soucie, W.G. The Ionic Modification of the Surface Charge and Isoelectric Point of Soy Protein. *J. Am. Oil Chem. Soc.* **1986**, *63*, 1346–1350. [[CrossRef](#)]
59. Buchheim, W. Aspects of Sample Preparation for Freeze-Fracture/Freeze-Etch Studies of Proteins and Lipids in Food Systems. A Review. *Food Struct.* **1982**, *1*, 9.
60. Gonzalez Ortiz, D.; Pochat-Bohatier, C.; Cambedouzou, J.; Bechelany, M.; Miele, P. Current Trends in Pickering Emulsions: Particle Morphology and Applications. *Engineering* **2020**, *6*, 468–482. [[CrossRef](#)]
61. Cinelli, G.; Cofelice, M.; Venditti, F. Veiled Extra Virgin Olive Oils: Role of Emulsion, Water and Antioxidants. *Colloids Interfaces* **2020**, *4*, 38. [[CrossRef](#)]
62. di Mattia, C.; Balestra, F.; Sacchetti, G.; Neri, L.; Mastrocola, D.; Pittia, P. Physical and Structural Properties of Extra-Virgin Olive Oil Based Mayonnaise. *LWT-Food Sci. Technol.* **2015**, *62*, 764–770. [[CrossRef](#)]
63. Sotiroidis, T.G.; Sotiroidis, G.T.; Varkas, N.; Xenakis, A. The Role of Endogenous Amphiphiles on the Stability of Virgin Olive Oil-in-Water Emulsions. *J. Am. Oil Chem. Soc.* **2005**, *82*, 415–420. [[CrossRef](#)]
64. Xenakis, A.; Papadimitriou, V.; Sotiroidis, T.G. Colloidal Structures in Natural Oils. *Curr. Opin. Colloid Interface Sci.* **2010**, *15*, 55–60. [[CrossRef](#)]
65. Venkataramani, D.; Tsulaia, A.; Amin, S. Fundamentals and Applications of Particle Stabilized Emulsions in Cosmetic Formulations. *Adv. Colloid Interface Sci.* **2020**, *283*, 102234. [[CrossRef](#)] [[PubMed](#)]
66. Frelichowska, J.; Bolzinger, M.A.; Chevalier, Y. Effects of Solid Particle Content on Properties of o/w Pickering Emulsions. *J. Colloid Interface Sci.* **2010**, *351*, 348–356. [[CrossRef](#)] [[PubMed](#)]
67. Tsabet, È.; Fradette, L. Effect of the Properties of Oil, Particles, and Water on the Production of Pickering Emulsions. *Chem. Eng. Res. Des.* **2015**, *97*, 9–17. [[CrossRef](#)]
68. Shah, B.R.; Li, Y.; Jin, W.; An, Y.; He, L.; Li, Z.; Xu, W.; Li, B. Preparation and Optimization of Pickering Emulsion Stabilized by Chitosan-Tripolyphosphate Nanoparticles for Curcumin Encapsulation. *Food Hydrocoll.* **2016**, *52*, 369–377. [[CrossRef](#)]
69. Li, X.L.; Liu, W.J.; Xu, B.C.; Zhang, B. Simple Method for Fabrication of High Internal Phase Emulsions Solely Using Novel Pea Protein Isolate Nanoparticles: Stability of Ionic Strength and Temperature. *Food Chem.* **2022**, *370*, 130899. [[CrossRef](#)]
70. Peng, W.; Kong, X.; Chen, Y.; Zhang, C.; Yang, Y.; Hua, Y. Effects of Heat Treatment on the Emulsifying Properties of Pea Proteins. *Food Hydrocoll.* **2016**, *52*, 301–310. [[CrossRef](#)]
71. Wang, Y.; Fan, B.; Tong, L.T.; Lu, C.; Li, S.; Sun, J.; Liu, L.; Wang, F. High Internal Phase Emulsions Stabilized Solely by Soy Protein Isolate. *J. Food Eng.* **2022**, *318*, 110905. [[CrossRef](#)]

72. Jiang, J.; Zhu, B.; Liu, Y.; Xiong, Y.L. Interfacial Structural Role of PH-Shifting Processed Pea Protein in the Oxidative Stability of Oil/Water Emulsions. *J. Agric. Food Chem.* **2014**, *62*, 1683–1691. [[CrossRef](#)] [[PubMed](#)]
73. Tavernier, I.; Patel, A.R.; van der Meeren, P.; Dewettinck, K. Emulsion-Templated Liquid Oil Structuring with Soy Protein and Soy Protein: κ -Carrageenan Complexes. *Food Hydrocoll.* **2017**, *65*, 107–120. [[CrossRef](#)]
74. Shao, Y.; Tang, C.H. Characteristics and Oxidative Stability of Soy Protein-Stabilized Oil-in-Water Emulsions: Influence of Ionic Strength and Heat Pretreatment. *Food Hydrocoll.* **2014**, *37*, 149–158. [[CrossRef](#)]
75. Gharsallaoui, A.; Cases, E.; Chambin, O.; Saurel, R. Interfacial and Emulsifying Characteristics of Acid-Treated Pea Protein. *Food Biophys.* **2009**, *4*, 273–280. [[CrossRef](#)]
76. Ghimire, B.K.; Seong, E.S.; Yu, C.Y.; Kim, S.H.; Chung, I.M. Evaluation of Phenolic Compounds and Antimicrobial Activities in Transgenic *Codonopsis lanceolata* Plants via Overexpression of the γ -Tocopherol Methyltransferase (γ -Tmt) Gene. *S. Afr. J. Bot.* **2017**, *109*, 25–33. [[CrossRef](#)]
77. Dmitrieva, A.; Vesnina, A.; Dyshlyuk, L. Antioxidant and Antimicrobial Properties of Squalene from *Symphytum officinale* and Chlorogenic Acid from *Trifolium pratense*. *AIP Conf. Proc.* **2022**, *2636*, 020005. [[CrossRef](#)]
78. Diamante, L.; Lan, T. Absolute Viscosities of Vegetable Oils at Different Temperatures and Shear Rate Range of 64.5 to 4835S-1. *J. Food Process.* **2014**, *3*. [[CrossRef](#)]
79. D'Alessio, G.; Flammini, F.; Faieta, M.; Pittia, P.; Di Mattia, C.D. Pea protein isolates: Emulsification properties as affected by preliminary pretreatments. *Ital. J. Food Sci.* **2022**, *34*, 25–32. [[CrossRef](#)]
80. Comas, D.I.; Wagner, J.R.; Tomás, M.C. Creaming stability of oil in water (O/W) emulsions: Influence of pH on soybean protein–lecithin interaction. *Food Hydrocoll.* **2006**, *20*, 990–996. [[CrossRef](#)]
81. Lam, A.C.Y.; Can Karaca, A.; Tyler, R.T.; Nickerson, M.T. Pea Protein Isolates: Structure, Extraction, and Functionality. *Food Rev. Int.* **2018**, *34*, 126–147. [[CrossRef](#)]
82. Jiang, L.; Wang, Z.; Li, Y.; Meng, X.; Sui, X.; Qi, B.; Zhou, L. Relationship between Surface Hydrophobicity and Structure of Soy Protein Isolate Subjected to Different Ionic Strength. *Int. J. Food Prop.* **2015**, *18*, 1059–1074. [[CrossRef](#)]
83. Wang, Z.; Li, Y.; Jiang, L.; Qi, B.; Zhou, L. Relationship between Secondary Structure and Surface Hydrophobicity of Soybean Protein Isolate Subjected to Heat Treatment. *J. Chem.* **2014**, *2014*, 1–10. [[CrossRef](#)]
84. Chang, C.Y.; der Jin, J.; Chang, H.L.; Huang, K.C.; Chiang, Y.F.; Ali, M.; Hsia, S.M. Antioxidative Activity of Soy, Wheat and Pea Protein Isolates Characterized by Multi-Enzyme Hydrolysis. *Nanomaterials* **2021**, *11*, 1509. [[CrossRef](#)]
85. Lanza, B.; Ninfali, P. Antioxidants in Extra Virgin Olive Oil and Table Olives: Connections between Agriculture and Processing for Health Choices. *Antioxidants* **2020**, *9*, 41. [[CrossRef](#)]
86. Naziri, E.; Mitić, M.N.; Tsimidou, M.Z. Contribution of Tocopherols and Squalene to the Oxidative Stability of Cold-Pressed Pumpkin Seed Oil (*Cucurbita pepo* L.). *Eur. J. Lipid Sci. Tech.* **2016**, *118*, 898–905. [[CrossRef](#)]
87. Rastrelli, L.; Passi, S.; Ippolito, F.; Vacca, G.; de Simone, F. Rate of Degradation of Alpha-Tocopherol, Squalene, Phenolics, and Polyunsaturated Fatty Acids in Olive Oil during Different Storage Conditions. *J. Agric. Food Chem.* **2002**, *50*, 5566–5570. [[CrossRef](#)] [[PubMed](#)]
88. Lin, C.-Z.; Zhu, C.-C.; Hu, M.; Wu, A.-Z.; Bairu, Z.-D.; Kangsa, S.-Q. Structure-Activity Relationships of Antioxidant Activity in Vitro about Flavonoids Isolated from *Pyrethrum tatsienense*. *J. Intercult. Ethnopharmacol.* **2014**, *3*, 123. [[CrossRef](#)]
89. Psomiadou, E.; Tsimidou, M. On the role of squalene in olive oil stability. *J. Agric. Food Chem.* **1999**, *47*, 4025–4032. [[CrossRef](#)] [[PubMed](#)]
90. Mateos, R.; Domínguez, M.M.; Luis Espartero, J.Á.; Cert, A. Antioxidant Effect of Phenolic Compounds, α -Tocopherol, and Other Minor Components in Virgin Olive Oil. *J. Agric. Food Chem.* **2003**, *51*, 7170–7175. [[CrossRef](#)] [[PubMed](#)]
91. Barouh, N.; Bourlieu-Lacanal, C.; Figueroa-Espinoza, M.C.; Durand, E.; Villeneuve, P. Tocopherols as Antioxidants in Lipid-Based Systems: The Combination of Chemical and Physicochemical Interactions Determines Their Efficiency. *Compr. Rev. Food Sci. Food Saf.* **2022**, *21*, 642–688. [[CrossRef](#)]
92. Frankel, E.N. The Antioxidant and Nutritional Effects of Tocopherols, Ascorbic Acid and Beta-Carotene in Relation to Processing of Edible Oils. *Bibl. Nutr. Dieta* **1989**, *43*, 297–312. [[CrossRef](#)]
93. Laguerre, M.; López Giraldo, L.J.; Lecomte, J.; Figueroa-Espinoza, M.C.; Baréa, B.; Weiss, J.; Decker, E.A.; Villeneuve, P. Chain Length Affects Antioxidant Properties of Chlorogenate Esters in Emulsion: The Cutoff Theory behind the Polar Paradox. *J. Agric. Food Chem.* **2009**, *57*, 11335–11342. [[CrossRef](#)]

Disclaimer/Publisher's Note: The statements, opinions and data contained in all publications are solely those of the individual author(s) and contributor(s) and not of MDPI and/or the editor(s). MDPI and/or the editor(s) disclaim responsibility for any injury to people or property resulting from any ideas, methods, instructions or products referred to in the content.